

MBB: Model-Based Baseline for Efficient Reinforcement Learning

Xubo Lyu¹, Site Li¹, Seth Siriya², Ye Pu², Mo Chen¹

Abstract—Model-free reinforcement learning (RL) is capable of learning control policies for high-dimensional, complex robotic tasks, but tends to be data-inefficient. Model-based RL and optimal control have been proven to be much more data-efficient if an accurate model of the system and environment is known, but can be difficult to scale to expressive models for high-dimensional problems. In this paper, we propose a novel approach to alleviate data inefficiency of model-free RL by warm-starting the learning process using a lower-dimensional model-based solutions. Particularly, we propose a baseline function that is initialized via supervision from a low-dimensional value function. Such a lower-dimensional value function can be obtained by applying model-based techniques on a low-dimensional problem featuring a known approximate system model. Therefore, our approach exploits the model priors from a simplified problem space implicitly and avoids the direct use of high-dimensional, expressive models. We demonstrate our approach on two representative robotic learning tasks and observe significant improvement in performance and efficiency, and analyze our method empirically with a third task.

I. INTRODUCTION

Model-free reinforcement learning (RL) has been successfully applied in games and robotics [1], [2] for solving complex, high-dimensional tasks. By mapping observations to actions via (deep) neural network [3], [4], model-free RL allows the control policies to be learned directly from high-dimensional inputs. However, model-free RL often requires an impractically large number of trials to learn desired behaviours which is costly and unrealistic especially in the context of robotics. To address such sample efficiency challenge, prior model-free RL methods incorporate techniques such as curiosity-based exploration [5], [6], curriculum learning [7], [8], while model-based RL methods try to incorporate environment model information into policy learning [9], [10].

Model-based methods learn and maintain a transition model of the domain environment online. Model-based RL achieves improved sample efficiency when it is able to learn a good model quickly [11], [12], but can perform poorly otherwise. Model-based RL is challenging in many high-dimensional robotic tasks especially when one aims to map sensor inputs directly to control actions, since the evolution of sensor inputs over time can be very difficult to model even using large, expressive neural networks [13], [14]. Such shortcomings can limit the model-based RL to relatively simple and low-dimensional tasks.

Optimal control has been widely used in various robotic applications [15]–[19]. It can be considered as a classical method in contrast to recent learning-based methods, and can provide solutions to many tasks without collecting any data from the environment, assuming an accurate system model is known. Optimal control lacks scalability to large-scale problems with high-dimensional state space especially when one aims to derive control policy from raw sensor input.

In this paper, we propose Model-Based Baseline (MBB), a novel approach that improves data efficiency of model-free RL on high-dimensional problems by leveraging solutions from associated low-dimensional problems. This is accomplished by initializing a baseline function for the RL algorithm in a supervised fashion, where the supervision is obtained by solving a low-dimensional problem with either value iteration, a model-based RL technique or model predictive control, an optimal control technique. In this way, our baseline implicitly incorporates the underlying model information of high-dimensional RL problems and is able to provide more preferable gradient estimation on policy update directions with fewer samples in certain challenging situations. Additionally, we propose a simple but useful criterion for updating the baseline accordingly to further facilitate the learning process.

We empirically evaluate our approach on two common mobile robotic tasks and obtain significant improvements in learning performance and efficiency, and analyze our approach with a third task. We choose Proximal Policy Optimization (PPO) [20] as a representative model-free algorithm to illustrate the effectiveness of our approach.

II. RELATED WORK

Initializing or warm-starting RL is a common technique to improve performance. To balance RL exploration against exploitation, optimistic value initialization [21], [22] has been proposed to initialize unseen states with higher values than the true values. Imitation learning has also been combined with RL through policy initialization via learning from demonstrations [23], [24]. Such demonstrations can come from humans or dynamical systems, and the initialized policy can be created through supervised learning or explicit programming [25], [26]. Our method can be regarded as a specific way to initialize the RL baseline function [27] with system dynamics priors.

Using a baseline function has been proved to be an effective variance reduction technique without introducing bias on policy gradient estimation, and has been widely studied [27]–[31]. The expected discounted return has been considered to be a good approximation of the optimal baseline [27] due to its lower variance, and has become a popular baseline choice in recent state-of-the-art actor critic RL methods [20], [30]. However, our work shows that the baseline that results in the lowest variance in policy gradient estimation may not always be the best choice in many complex tasks especially when a large amount of exploration is needed (e.g. sparse reward). In contrast, our formulation of baseline function incorporates system priors from a simplified problem and drastically speeds up the RL process in complex robotic tasks with sparse reward.

Combining optimal control and RL has the potential to inherit the benefits of both techniques. In [32], [33], model predictive control (MPC) has been employed to either generate guided training data or provide trajectory optimization-based supervision for RL to learn complex, high-dimensional

¹School of Computing Science, Simon Fraser University, BC, CA, V5A1S6. xly@sfu.ca; sitel@sfu.ca; mochen@cs.sfu.ca

²Department of Electrical and Electronic Engineering, The University of Melbourne, Vic 3010 AU. ssiriya@student.unimelb.edu.au; ye.pu@unimelb.edu.au

policies. Within the curriculum RL framework, reachability theory has been applied to provide a more intuitive, accurate criterion for curriculum generation [34]. Recently, the authors of [35] presented an approach to shape an effective RL reward function by solving time-to-reach (TTR), a classical optimal control problem. Our approach aims to improve sample efficiency by leveraging solutions from lower-dimensional problems produced by optimal control to facilitate the learning of high-dimensional RL policies.

III. PRELIMINARIES

A. RL Notations and Terminologies

Consider a Markov Decision Process (MDP) with an agent and environment state S , a set of agent actions A , a probability of transition (at any time t) from state s to state s' under action a : $P_a(s, s') = \Pr(s_{t+1} = s' | s_t = s, a_t = a)$ and an immediate reward $r(s_t, a_t)$. In this paper, we simplify the reward function as $r(s_t)$ so that it only depends on current state s_t . To match notations of the approximate system dynamics discussed in Sec. IV, we introduce a slight abuse of notation $s_{t+1} \sim f(s_t, a_t)$ to denote that s_{t+1} is drawn from the distribution $\Pr(s_{t+1} = s' | s_t = s, a_t = a)$.

The policy $\pi(a|s)$ specifies the probability of action a that the agent will choose in state s . The trajectory τ is a sequence of states and actions $\tau = (s_0, a_0, s_1, a_1, \dots)$ in the environment, and the discounted return $R(\tau) = \sum_{t=0}^{\infty} \gamma^t r(s_t)$ specifies the discounted sum of all rewards obtained by the agent, with $\gamma \in [0, 1]$ denoting a discount factor controlling the importance of long-term reward. We also denote on-policy value function as $V^\pi(s)$, which gives the expected return starting in state s and always acting according to policy π .

Given an MDP, we aim to find a policy π to maximize the expected return $J(\pi) = \mathbb{E}_{\tau \sim \pi} [R(\tau)]$.

B. Actor-Critic RL

Policy gradient methods maximize the expected return $J(\pi)$ by repeatedly estimating its gradient with respect to policy parameters θ and use it to directly update the policy $\pi_\theta(a|s)$ via stochastic gradient ascent: $\theta_{k+1} = \theta_k + \alpha \nabla_\theta J(\pi_{\theta_k})$. Actor-critic methods, as an important class of policy gradient methods, aim to obtain better policy gradient estimates by concurrently updating a policy $\pi(a|s)$ (actor) and a value function $V^\pi(s)$ (critic) corresponding to π . Intuitively, the critic is used to evaluate the actor and drive the actor's policy parameters in the direction of performance improvement. In this paper, we assume a generic form of policy gradient [30] given by Eq. (1),

$$\nabla_\theta J(\pi_\theta) = \mathbb{E}_{\tau \sim \pi_\theta} \left[\sum_{t=0}^T \nabla_\theta \log \pi_\theta(a_t | s_t) \left(G_t^\lambda - b(s_t) \right) \right], \quad (1)$$

where G_t^λ is the TD(λ) return [36] considering weighted average of n -step returns for $n = 1, 2, \dots, \infty$ via parameter λ .

C. Baseline in Policy Gradient Estimation

In Eq. (1), $b(s_t)$ is called baseline¹ and it potentially reduces the variance without changing the expectation of policy gradient estimation [27]. One common choice of $b(s_t)$ in actor-critic RL is the on-policy value function $V^\pi(s_t)$ that approximates the expected return, which provides almost the

¹To avoid ambiguity, we use the term ‘‘baseline’’ to refer to the function $b(\cdot)$ used in policy gradient estimation in Eq. (1) and the term ‘‘baseline approach’’ to represent a method to which we will compare in Sec. V.

lowest variance [27]. In general, actor-critic RL initialize $V^\pi(s_t)$ randomly and update it by constantly solving a nonlinear regression problem $\min_\phi \sum_{t=1}^T \left\| V_\phi^\pi(s_t) - G_t^\lambda \right\|^2$, where ϕ are on-policy value function parameters. Empirically, the choice $b(s_t) = V^\pi(s_t)$ results in more stable policy learning compared to other choices. However, as we will demonstrate, this may not always be the best choice, especially when a large amount of exploration is needed.

D. Value Iteration

The value function V^π corresponding to any policy π can be computed by iteratively applying Bellman expectation backup [37] until it converges, as shown in Eq. (2) where k is iteration index. This procedure is a form of value iteration, a classical dynamic programming-based method that is often applied in discrete and low-dimensional state spaces.

$$V_{k+1}(s) = \sum_{a \in A} \pi(a|s) (r(s, a) + \gamma \sum_{s' \in S} P(s'|s, a) \cdot V_k(s')) \quad (2)$$

The computational complexity of value iteration restricts its use on many complicated RL tasks despite the theoretical guarantee on the convergence to global optimality. However, our work takes advantage of the global optimality by using value function to solve the low-dimensional problems and incorporates resulting value function into the baseline of the high-dimensional RL tasks. The choice of π in Eq. (2) is flexible considering the balance between RL exploration and exploitation. Instead of using the greedy (optimal) policy, we use the Boltzmann policy [38] in this paper.

E. Model Predictive Control

Model Predictive Control (MPC) uses a model of a system to predict the system's future behaviours and optimizes a given cost function, possibly subject to input and state constraints [39], [40]. Specifically, MPC repeatedly solves a constrained planning problem with a look-ahead horizon H at each time step t and only executes the first element of the control sequence obtained. Note that for most RL problems, one can define related MPC problems and solve it assuming a known system model.

In addition to value iteration, we take the MPC solutions of a simplified problem with a lower-dimensional system model, and map it to the baseline of high-dimensional RL task. The use of MPC scales our approach to the problems of which even the simplified system models remain too high dimensional to be tractably solved by value iteration.

IV. MODEL-BASED BASELINE

In this paper, we propose a model-informed baseline function that can be a substitute for on-policy value function $V^\pi(\cdot)$ as a novel baseline to facilitate policy gradient-based RL. It is worth noting that the primary purpose of our baseline is not to minimize variance of gradient estimation as $V^\pi(\cdot)$ does, but to give better policy update directions with fewer samples in certain challenging situations.

Before proceeding, we first introduce necessary notations and terminologies used in this section. We use the phrase ‘‘full MDP model’’ to refer to the state transition $f(\cdot)$ in the high-dimensional target RL problem Ω . For every Ω , we denote its counterpart, a simplified, low-dimensional problem as $\tilde{\Omega}$, which involves an approximate, low-dimensional model $\tilde{f}(\cdot)$. We denote the on-policy value function of the actor-critic RL for the problem Ω as $V_\phi^\pi(\cdot)$ and its corresponding

policy as $\pi_\theta(\cdot)$. Additionally, we denote our baseline function for the problem Ω as $V_\eta^M(\cdot)$, which is initialized via the value solutions $\tilde{V}^M(\cdot)$ of a low-dimensional problem $\tilde{\Omega}$. ϕ, θ, η represent function parameters. We use the term ‘‘warm-start’’ to refer to the operations of obtaining the low-dimensional value solutions and initializing the model-based baseline.

We now present our Model-Based Baseline (MBB) approach². Our algorithm starts with choosing an approximate system model $\tilde{f}(\cdot)$, which should be relatively low-dimensional but captures the key system behaviors of full MDP $f(\cdot)$ in the target RL problem Ω . Then, we employ either model-based RL (value iteration) or optimal control (MPC) to solve the simplified problem $\tilde{\Omega}$ that features $\tilde{f}(\cdot)$ to collect training data $\mathcal{D} := \{(s_i, \tilde{V}^M(\tilde{s}_i))\}$. \mathcal{D} contains the mapping between states in Ω and approximate values in $\tilde{\Omega}$, and is used to train the model-based baseline $V_{\eta_0}^M(\cdot)$. Starting with the randomly initialized policy π_{θ_0} , we begin updating θ_0 with any actor-critic RL algorithms using our baseline $V_{\eta_0}^M(\cdot)$. At each iteration k , we use the policy gradient \hat{g}_k obtained from online trajectories \mathcal{T}_k to update policy θ_k , and optionally update the baseline parameter η_k based on a novel criterion. Algorithm 1 summarizes our method.

Algorithm 1 MBB: Model-Based Baseline

- 1: Select an approximate model $\tilde{f}(\cdot)$ for the target RL problem Ω and a corresponding simplified problem $\tilde{\Omega}$ modelled by $\tilde{f}(\cdot)$.
 - 2: Apply value iteration or MPC to $\tilde{\Omega}$ to collect training dataset $\mathcal{D} := \{(s_i, \tilde{V}^M(\tilde{s}_i))\}$ for state-value mapping.
 - 3: Initialize the model-based baseline $V_{\eta_0}^M$ via supervised learning on \mathcal{D} . Initialize policy π_{θ_0} randomly.
 - 4: **for** $k = 0, 1, 2, \dots$ **do**
 - 5: Collect trajectories $\mathcal{T}_k = \{\tau_i | i = 0, 1, 2, \dots\}$ by running policy $\pi_k = \pi_{\theta_k}$ in target RL domain.
 - 6: Calculate TD(λ) return G_t^λ and the model-based baseline function $V_{\eta_0}^M(s_t)$ for every s_t to estimate policy gradient \hat{g}_k based on Eq. (1).
 - 7: Update policy $\theta_{k+1} = \theta_k + \alpha_k \hat{g}_k$.
 - 8: Update model-based baseline parameter η_k based on the criterion defined in Eq. (8) and Eq. (9).
 - 9: **end for**
-

A. Model Selection

‘‘Model selection’’ refers to choosing an approximate, low-dimensional system model for the target RL task and compute value function based on it. The full MDP model $f(\cdot)$ is often inaccessible since it captures the evolution of high-dimensional state inputs including both sensor data and robot internal state. However, an approximate system model $\tilde{f}(\cdot)$ is often known and accessible. The tilde implies it is not necessary for $\tilde{f}(\cdot)$ to perfectly reflect the real state transitions $f(\cdot)$. In fact, $\tilde{f}(\cdot)$ should typically be lower-dimensional to allow for efficient value computation, while still capturing key robot physical dynamics.

The connection between the full MDP model and the approximate system model is formalized via the state, as shown in Eq. (3). Here we define a bijective function \mathcal{F} to establish a one-to-one correspondence between \tilde{s} and s . Particularly, in this paper we consider \mathcal{F} to be a selection matrix mapping denoted by \mathbf{M} , which can be chosen based on system knowledge to ensure that \tilde{s} captures the key aspects of robot physical dynamics. Therefore, the approximate

system state \tilde{s} is a subset of the full MDP state s : $s = (\tilde{s}, \hat{s})$ where \hat{s} denotes state components in the full MDP model that are not part of \tilde{s} .

$$\tilde{s} = \mathcal{F}(s) = \mathbf{M}s \quad (3)$$

The approximate system state \tilde{s} evolves according to a known, low-dimensional model \tilde{f} , where \tilde{f} can be in the form of ODE as in Eq. (4a) or MDP as in Eq. (4b), or any other model as long as there is a method to efficiently solve the lower-dimensional problem.

$$\dot{\tilde{s}}(t) = \tilde{f}(\tilde{s}(t), \tilde{a}(t)) \quad (4a)$$

$$P_{\tilde{a}}(\tilde{s}_t, \tilde{s}_{t+1}) = \Pr(\tilde{s}_{t+1} | \tilde{s}_t, \tilde{a}_t) \quad (4b)$$

For example, in the simulated car example shown in Sec. V-A, the full state $s = (x, y, \theta, v, w, d_1, \dots, d_8)$ includes the position (x, y) , heading θ , speed v , turn rate w , as well as eight laser range measurements d_1, \dots, d_8 that provide distances from nearby obstacles. As one can imagine, the evolution of s can be very difficult if $f(\cdot)$ is impossible to obtain, especially in a *a priori* unknown environment.

By following Eq. (3) and choosing the selection matrix $\mathbf{M} = [\mathbf{I}_{3 \times 3} \quad \mathbf{0}_{3 \times 10}]$, the state of the approximate system \tilde{s} can be constructed to contain a subset of the internal state (x, y, θ) , and evolves according to Eq. (4). In particular, for the simulated results of the car, we choose the Dubins Car model to be the approximate system dynamics given in Eq. (5). As we will show, such simple dynamics are sufficient for improving data efficiency in model-free RL. With this choice, the remaining state $\hat{s} = (v, w, d_1, \dots, d_8)$.

$$\dot{\tilde{s}} = \begin{bmatrix} \dot{x} \\ \dot{y} \\ \dot{\theta} \end{bmatrix} = \begin{bmatrix} v \cos \theta \\ v \sin \theta \\ \omega \end{bmatrix} \quad (5) \quad \dot{\hat{s}} = \begin{bmatrix} \dot{v} \\ \dot{w} \\ \dot{d}_1 \\ \vdots \\ \dot{d}_8 \end{bmatrix} = \begin{bmatrix} v \cos \theta \\ v \sin \theta \\ \omega \\ \alpha_v \\ \alpha_w \\ \alpha_{d_1} \\ \vdots \\ \alpha_{d_8} \end{bmatrix} \quad (6)$$

The choice of the approximate system model representing the real robot may be very flexible, depending on what behaviour one wishes to capture. In the 3D ODE model given in Eq. (5), we focus on modelling the position and heading of the car to be consistent with the goal. However, if speed and angular speed are deemed crucial for the task under consideration, one may also choose a more complex 5D approximate system given in Eq. (6), where we have $\tilde{s} = (x, y, \theta, v, \omega)$, and $\hat{s} = (d_1, \dots, d_8)$. To re-iterate, we may choose \tilde{s} such that a reasonable explicit, closed-form model $\tilde{f}(\cdot)$ can be derived. And a good choice of approximate model should be computationally tractable for the value function computation, and captures the system behaviours that are important for performing the desired task.

B. Training Data Generation

We generate training data $\{s_i, \tilde{V}^M(\tilde{s}_i)\}$ to train a model-based baseline $V^M(s)$ for the target RL problem. The state s_i can be obtained by directly sampling from the full MDP problem Ω . $\tilde{V}^M(\tilde{s}_i)$ is obtained by plugging in \tilde{s}_i into $\tilde{V}^M(\cdot)$, which can be computed using model-based techniques such as value iteration or MPC. We now outline two examples.

1) **Value Iteration Solution as Ground Truth:** We first consider the simple case, where the robotic system can be described via a sufficiently low-dimensional (normally no more than 4D) model. This is because value iteration is a dynamic programming-based method, whose computational complexity scales exponentially with system dimensionality.

For instance, a differential drive robot in this work can be modelled as a 3D system using Eq. (5). To apply

²Code and supplementary material of our paper are available: https://github.com/SFU-MARS/SL_optCtrl

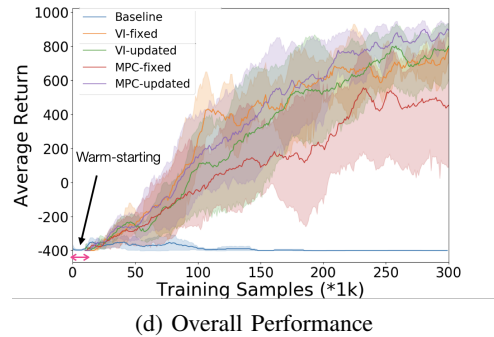
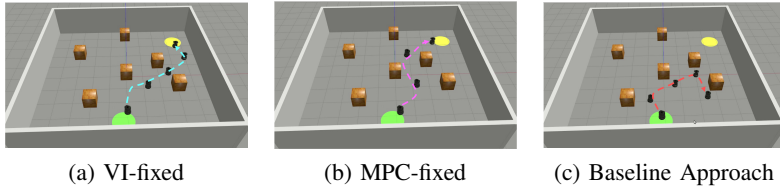


Fig. 1: Simulated car trajectories at iteration 90 from (a) VI-fixed (b) MPC-fixed and (c) Baseline approach. Both variants of MBB approach successfully learn a collision-free, goal-reaching policy while the baseline approach learns to conservatively move in free space while avoiding obstacles but never getting to the goal. (d) Overall performance comparison on the car example. The black arrow refers to MBB warm-starting period, which is approximately 10K training samples. During this period the baseline approach starts RL process while MBB does not. Including this results in a fair comparison on learning efficiency between the baseline and MBB approach.

value iteration on it, we apply discretization on the state $\tilde{s} = (x, y, \theta)$ and action $\tilde{a} = (v, \omega)$ space, and repeatedly calculate the value for each discrete state \tilde{s} following Eq. (2) until convergence. Then, we randomly sample a large number of s_i , and compute their $\tilde{V}^M(\tilde{s}_i)$ accordingly to obtain the training dataset $\{s_i, \tilde{V}^M(\tilde{s}_i)\}$.

2) **MPC Solution as Ground Truth:** Many complex robotic systems cannot be represented as models with its dimensionality low enough for tractable value iteration. A quadrotor is one example. Describing the dynamics of a planar quadrotor typically requires a 6D nonlinear dynamics, which is quite difficult to solve using value iteration. In this case, we propose to use an MPC-aided, sampling-based approximation to estimate the value for such 6D state space. The full version MPC problem and the 6D quadrotor model can be found in [41].

A number of initial states are generated by uniformly sampling over the entire 6D state space $\tilde{s} = (x, v_x, z, v_z, \theta, \omega)$. Next, we utilize MPC to calculate the solutions of the low-dimensional quadrotor problem given each of the initial states using the 6D approximate model and specifying necessary domain constraints such as obstacles. This allows for collection of ample feasible and infeasible trajectories over the entire 6D state space. The set of trajectories are denoted as $\{\tilde{\tau}_k | k = 0, 1, 2, \dots, N\}$. For each trajectory $\tilde{\tau}_k$ with the horizon of length H_k , we take every state $\tilde{s}_i, i \in \{0, 1, 2, \dots, H_k - 1\}$ in it and re-map it to s_i by retrieving the remaining state \hat{s}_i via simulation, and compute $\tilde{V}^M(\tilde{s}_i)$ following Eq. (7), where $r(\cdot)$ is the reward function of the target RL problem Ω .

$$\tilde{V}^M(\tilde{s}_i) = \sum_{t=0}^{H_k} \gamma^t r(s_t) \quad (7)$$

C. Model-based Baseline for Actor-critic RL

We establish a nonlinear approximator using neural network to represent $V^M(\cdot)$ and optimize its parameters via supervised learning given the data set $\mathcal{D} = \{(s_i, \tilde{V}^M(\tilde{s}_i))\}$. We choose mean squared error (MSE) as loss function. Once $V^M(\cdot)$ is initialized using \mathcal{D} , we can treat it as a model-based baseline and easily integrate it into most of actor-critic RL algorithms. This is in contrast to the commonly-used baseline $V^\pi(\cdot)$ in Eq. (1), which is normally randomly initialized. Therefore, the RL optimization starts as usual, except with the key system information implicitly involved.

The TD(λ) return G_t^λ in Eq. (1) needs to be estimated based on a batch of collected trajectories. In our main results

in Sec. V, we take $\lambda = 1$ to use TD(1) (a.k.a. Monte-Carlo) return as an unbiased estimation. For the general choices of $\lambda \in [0, 1)$, bias can be introduced to the return estimation since we need to employ a value function ($V^\pi(\cdot)$ or $V^M(\cdot)$) to calculate G_t^λ . However, as we will show in [41], we still observe similar benefits of learning efficiency as when we use Monte-Carlo return despite such bias.

Additionally, we propose a criterion for optionally updating $V^M(\cdot)$ using Eq. (8). At each iteration, we use Eq. (8a) to calculate the averaged Monte-Carlo return $\overline{G^1}$ and Eq. (8b) to calculate the averaged value prediction $\overline{G^{VM}}$ provided by our baseline $V^M(\cdot)$ over a batch of trajectories \mathcal{T} . $|\mathcal{T}|$ is the number of trajectories and s_0 in Eq. (8b) refers to the starting state of each trajectory. Then we update the baseline $V^M(\cdot)$ using Eq. (9) only if $\overline{G^1} \geq \overline{G^{VM}}$.

$$\overline{G^1} = \frac{1}{|\mathcal{T}|} \sum_{\tau \in \mathcal{T}} \sum_{t=0}^T \gamma^t r(s_t) \quad (8a)$$

$$\overline{G^{VM}} = \frac{1}{|\mathcal{T}|} \sum_{\tau \in \mathcal{T}} V^M(s_0) \quad (8b)$$

Such a criterion considers our model-based baseline $V^M(\cdot)$ as a special critic to evaluate current policy π . It guarantees that the critic will get updated only if the roll-outs indicate more favourable performance compared to what the initialized critic suggests. Such a critic $V^M(\cdot)$ will behave more robustly compare to $V^\pi(\cdot)$ even though the initial policy is performing very poorly.

$$\eta_{k+1} = \arg \min_{\eta_k} \frac{1}{|\mathcal{T}_k| T} \sum_{\tau \in \mathcal{T}_k} \sum_{t=0}^T (V_{\eta_k}^M(s_t) - G_t^1)^2 \quad (9)$$

V. EXPERIMENTAL RESULTS

In this section, we compare the performance of the baseline approach with our MBB approach. The baseline approach refers to using the PPO algorithm with randomly initialized on-policy value function $V^\pi(\cdot)$ as baseline and employing regular value update rule, as discussed in Sec. III-B; while the MBB approach refers to the use of PPO algorithm but with the model-based baseline $V^M(\cdot)$ initialized from the value solutions of an approximate system model, as described in Sec. IV. Note that MBB includes four variants: **VI-fixed**, **VI-updated**, **MPC-fixed** and **MPC-updated**, depending on the use of value iteration or MPC. Additionally, “fixed” refers to the baseline function remains unchanged once initialized while “updated” means the baseline function

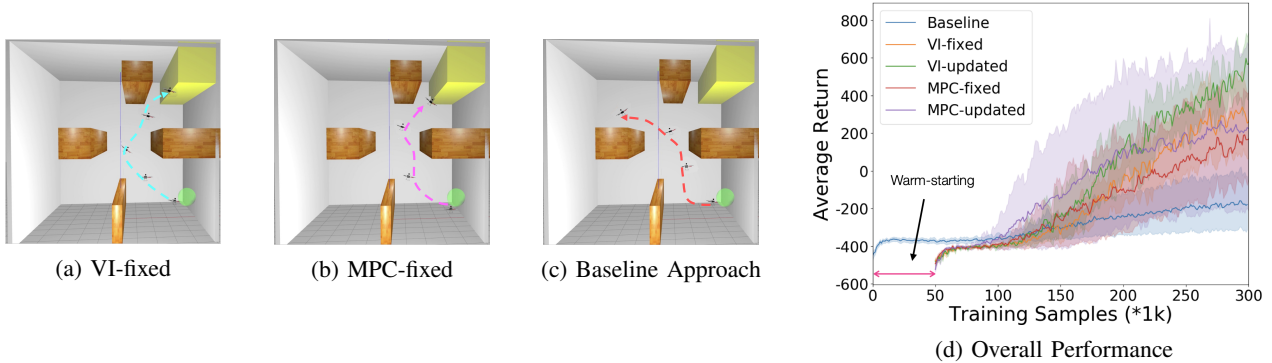


Fig. 2: Simulated quadrotor trajectories at iteration 200 from (a) VI-fixed (b) MPC-fixed and (c) Baseline approach. Our approach learns to fly to the goal yet the baseline approach keeps failing in a undesired (upper-left) area and never recovers. (d) Overall performance comparison on the quadrotor example, with the sample cost at approximately 50K of MBB warm-starting stage included.

will be updated based on Eq. (8) and Eq. (9). Without loss of generality, we employ sparse reward [41] for all examples.

A. Differential Drive Car

We first apply our approach on a simulated TurtleBot, which resembles a differential drive car navigating in an environment with multiple static obstacles. The goal of this task is to learn a control policy for the car to move from a starting area (green area in Fig. 1) to a specific goal area (yellow area in Fig. 1) following a collision-free trajectory. The car starts with randomly-sampled positions and angles from the starting area $S_b = \{(x, y, \theta) | -0.5 \text{ m} \leq x \leq 0.5 \text{ m}; -3.5 \text{ m} \leq y \leq -2.5 \text{ m}; 0 \leq \theta \leq \pi\}$, and aims to arrive at the goal, which is defined as a 3D region $S_g = \{(x, y, \theta) | 3.7 \text{ m} \leq x \leq 4.3 \text{ m}; 3.7 \text{ m} \leq y \leq 4.3 \text{ m}; 0.45 \text{ rad} \leq \theta \leq 1.05 \text{ rad}\}$. The state and observation of this example are discussed in Sec. IV-A. The car moves by controlling the speed and turn rate. Note that the robot is not aware of the environment in advance but needs to learn a control policy purely from trial and error. In our approach, we initialize the model-based baseline by applying value iteration or MPC on a lower-dimensional, approximate car system in Eq. (5) which only considers (x, y, θ) as state and angular velocity ω as control.

Fig. 1d shows the learning progresses for different approaches. We take the averaged training return versus iterations as performance measurement. Results are summarized across 10 different trials. The curves show the mean return and the shaded area represents the standard deviation of 10 trials. As evident from Fig. 1d, all variants of our approach continue to improve as the learning progresses and eventually significantly outperforms the baseline approach. In terms of policy behaviours shown in Fig. 1a, 1b and 1c, our approach can successfully learn collision-free paths despite the collisions in the earlier stage while the baseline approach only learns highly conservative behaviours such as staying around the same area after many failures.

Fig. 1d takes the warm-starting stage required by MBB approach into account for a fair comparison of learning efficiency in terms of sample and computational cost. As summarized in Table. I, the car example only requires 10K samples and 5.5% computational time for MBB warm-starting, which is insignificant compared to that of entire RL process, indicating the efficiency of MBB over the baseline approach. The data in Table. I is measured on the hardware: Intel(R) Core(TM) i7-8700K CPU@3.70GHz; RAM 32GB.

In this example, value iteration is shown to be a better technique compared to MPC for MBB approach. This makes sense as value iteration exhausts all possible state combinations of the low-dimensional system while MPC produces a finite set of locally optimal trajectories. With both value iteration and MPC, allowing baseline update further improves performance. This is especially true with MPC. This indicates the necessity of introducing an appropriate update criterion. Intuitively, keeping a well-initialized baseline function fixed would be advantageous in preventing policy getting stuck in the early stage; however, eventually such fixed baseline may become somewhat detrimental and can prevent further policy improvement.

Examples	Types	Cost	
		Sample	Computation(%)
Car	Value Iteration	10K	5.5
Quadrotor	MPC	50K	29.2

TABLE I: Cost of warm-starting period of the MBB approach on differential car and planar quadrotor examples. Sample cost is measured by the number of timesteps that the agent interacts with the environment during the amount of time needed for warm-starting. Computational cost is represented by the wall time percentage that warm-starting occupies compared to that of total RL training process, under equivalent computing configuration.

B. Planar Quadrotor

In the second example, we select a planar quadrotor as a more complicated system to test our approach. The control of a quadrotor is usually considered challenging due to its under-actuated nature and the fact that its translational movement partly depends on its orientation. Therefore, the goal of this experiment is to validate that our MBB approach still works well even on a highly dynamic and unstable system. “Planar” means the quadrotor is restricted to move in the vertical (x - z) plane by changing the pitch without affecting the roll and yaw.

The simulated setup is shown in Fig. 2 with starting region $S_b = \{(x, z, \psi) | 2.5 \text{ m} \leq x \leq 3.5 \text{ m}; 2.5 \text{ m} \leq z \leq 3.5 \text{ m}; -\pi/4 \leq \psi \leq \pi/4\}$ (green area) and goal region $S_g = \{(x, z, \psi) | 3.5 \text{ m} \leq x \leq 4.5 \text{ m}; 8.5 \text{ m} \leq z \leq 9.5 \text{ m}; 0 \leq \psi \leq \pi/3\}$ (yellow area). To use MBB approach, we choose the approximate system model from [41] with a 6-dimensional internal state $\tilde{s} = (x, v_x, z, v_z, \psi, \omega)$, where x, z, ψ denote the planar positional coordinates

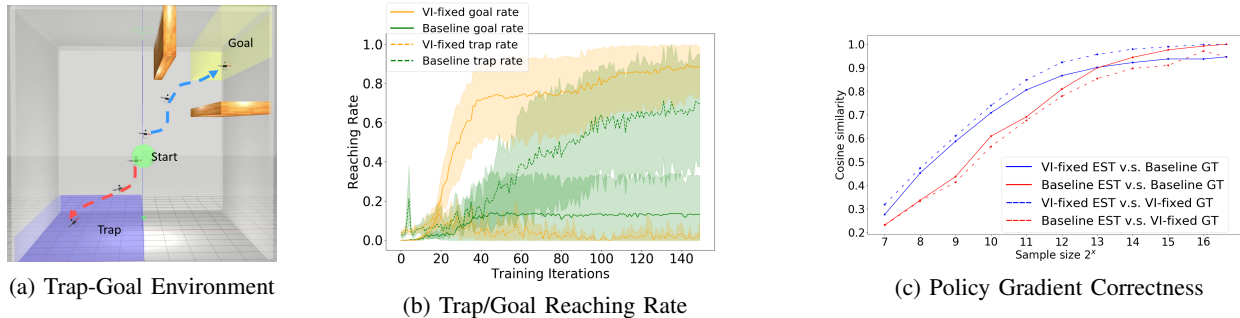


Fig. 3: **(a)** Quadrotor trajectories in the Trap-Goal environment using MBB (blue dashed line) and the baseline approach (red dashed line). **(b)** The training performance of MBB and the baseline approach in terms of goal and trap reaching rate. **(c)** The comparison of policy gradient estimation correctness between using MBB and the baseline approach.

and pitch angle, and v_x, v_z, ω denote their time derivatives respectively. The quadrotor receives full state $s = (x, v_x, z, v_z, \psi, \omega, d_1, \dots, d_8)$, which contains eight sensor readings extracted from the laser range finder for detecting obstacles, in addition to the internal state \tilde{s} . The quadrotor intends to learn a policy mapping from states and observations to its two thrusts F_1 and F_2 that lead it to the goal.

Fig. 2d depicts the evaluation of our approach as well as the baseline approach on the planar quadrotor, in a similar way as the car example. Compared to the car, the quadrotor is harder to control due to its unstable physical nature thereby leading to slightly inferior performance in general. Despite the computational complexity, we still apply value iteration on the 6D approximate state space to fully test our approach on complex systems. The average returns from the four variants of our approach start outperforming the baseline approach at 150 iteration. In contrast with MPC-based technique, value iteration ends up with the best performance and much lower variance, indicating its notable advantage in giving accurate, robust value supervision. However, it is worth noting that the MPC based technique retains more scalability to relatively complex systems without losing too much learning performance. Moreover, although MPC-based warm-starting on the quadrotor requires higher sample and computational cost than the car as shown in Table. I, the overall learning efficiency is still significantly improved.

The trajectories plots also highlight the efficiency of our approach. As evident in Fig. 2c, the baseline approach fails to find the correct path and gets stuck in an undesirable region. This is potentially because the baseline approach forces its baseline (on-policy value function $V^\pi(\cdot)$) to be constantly updated towards policy return, and this can result in near-zero advantage estimation [30] and restrain further policy exploration, which is especially unfavourable to an initially poorly performing policy. In contrast, the variants of our approach can avoid such issue by leveraging approximate model priors to construct model-based baseline $V^M(\cdot)$ and applying proper baseline update criterion. Therefore, our approach tractably and reliably learns a policy that smoothly and successfully reaches the goal.

VI. DISCUSSION: POLICY GRADIENT CORRECTNESS

In this section, we investigate the correctness of RL policy gradient estimation for a “Trap-Goal” environment to gain insight on why our approach is able to improve learning efficiency. Additional analysis on the advantage estimation and gradient variance can be found in [41]. We take **VI-fixed** as a representative variant of our MBB approach.

To highlight the importance of correct gradient estimation in RL tasks, we purposely design an example shown in Fig. 3a, which contains a goal (yellow area) and trap (purple area) that give positive but various rewards (+1000 for goal, +100 for trap) such that the correct policy gradient should drive the policy towards reaching the goal despite possible misleading gradients caused by the trap.

Fig. 3a depicts trajectories by executing policies learned from MBB and the baseline approach. Under same exploration strategy, the baseline approach leads to a trap-reaching policy (red dashed line) while MBB approach learns the desired goal-reaching policy (blue dashed line). This result is also reflected in Fig. 3b where MBB approach has an increasing goal-reaching rate as learning progresses while the baseline approach has an increasing trap-reaching rate.

Fig. 3c statistically illustrates the correctness comparison of policy gradient estimation between MBB and the baseline approach, in terms of cosine similarity versus sample size. We denote **baseline GT** and **VI-fixed GT** as two types of policy gradient ground truths that are computed by the baseline and MBB approach respectively. We do so by calculating Eq. (1) over infinite samples³ collected by running a fixed policy π . Correspondingly, with $N(N \leq N_{\max})$ samples, we obtain two types of gradient estimation named **baseline EST** and **VI-fixed EST**. We then compute the cosine similarity between **baseline EST/VI-fixed EST** and two ground truths respectively with multiple choices of sample size N and plot the results in Fig. 3c. The results are averaged over 100 random selections of N samples. Featuring with higher cosine similarity, our approach (blue solid and dashed lines) leads to more accurate gradient estimation than the baseline approach in terms of gradient direction, regardless of sample size or ground truth type, especially at relatively low N .

VII. CONCLUSION

We propose Model-Based Baseline, a novel approach to alleviate the data inefficiency of model-free RL by implicitly leveraging model priors. This is achieved by first solving a simplified, lower-dimensional version of the RL problem using model-based methods, which allows the use of known approximate system models. The lower-dimensional value solutions are then used to warm-start a baseline function which can act as a critic for the target high-dimensional RL problem. The results show that our approach can accelerate learning by taking advantage of a known, approximate model yet still retain the flexibility of model-free RL.

³In practice, we select a relatively large number $N_{\max} = 102,400$ instead of infinity samples to compute the ground truth.

REFERENCES

- [1] V. Mnih, K. Kavukcuoglu, D. Silver, A. Graves, I. Antonoglou, D. Wierstra, and M. Riedmiller, "Playing atari with deep reinforcement learning," *arXiv preprint arXiv:1312.5602*, 2013.
- [2] N. O. Lambert, D. S. Drew, J. Yaconelli, S. Levine, R. Calandra, and K. S. Pister, "Low-level control of a quadrotor with deep model-based reinforcement learning," *IEEE Robotics and Automation Letters*, vol. 4, no. 4, pp. 4224–4230, 2019.
- [3] R. S. Sutton, D. A. McAllester, S. P. Singh, and Y. Mansour, "Policy gradient methods for reinforcement learning with function approximation," in *Advances in neural information processing systems*, 2000, pp. 1057–1063.
- [4] J. Schulman, S. Levine, P. Abbeel, M. Jordan, and P. Moritz, "Trust region policy optimization," in *International conference on machine learning*, 2015, pp. 1889–1897.
- [5] D. Pathak, P. Agrawal, A. A. Efros, and T. Darrell, "Curiosity-driven exploration by self-supervised prediction," *2017 IEEE Conference on Computer Vision and Pattern Recognition Workshops (CVPRW)*, pp. 488–489, 2017.
- [6] Y. Burda, H. A. Edwards, D. Pathak, A. J. Storkey, T. Darrell, and A. A. Efros, "Large-scale study of curiosity-driven learning," *ArXiv*, vol. abs/1808.04355, 2019.
- [7] Y. Bengio, J. Louradour, R. Collobert, and J. Weston, "Curriculum learning," in *Proc. Annual Int. Conf. Machine Learning*, 2009.
- [8] C. Florensa, D. Held, M. Wulfmeier, and P. Abbeel, "Reverse curriculum generation for reinforcement learning," *CoRR*, 2017. [Online]. Available: <http://arxiv.org/abs/1707.05300>
- [9] T. Hester and P. Stone, "Learning and using models," in *Reinforcement Learning: State of the Art*, M. Wiering and M. van Otterlo, Eds. Berlin, Germany: Springer Verlag, 2011.
- [10] D. Silver, A. Huang, C. J. Maddison, A. Guez, L. Sifre, G. Van Den Driessche, J. Schrittwieser, I. Antonoglou, V. Panneershelvam, M. Lanctot *et al.*, "Mastering the game of go with deep neural networks and tree search," *nature*, vol. 529, no. 7587, p. 484, 2016.
- [11] A. Nagabandi, G. Kahn, R. S. Fearing, and S. Levine, "Neural network dynamics for model-based deep reinforcement learning with model-free fine-tuning," *2018 IEEE International Conference on Robotics and Automation (ICRA)*, pp. 7559–7566, 2018.
- [12] T. Kurutach, I. Clavera, Y. Duan, A. Tamar, and P. Abbeel, "Model-ensemble trust-region policy optimization," in *International Conference on Learning Representations*, 2018. [Online]. Available: <https://openreview.net/forum?id=SJinbWRZ>
- [13] M. P. Deisenroth and C. E. Rasmussen, "Reducing model bias in reinforcement learning," 2010.
- [14] E. Langlois, S. Zhang, G. Zhang, P. Abbeel, and J. Ba, "Benchmarking model-based reinforcement learning," *arXiv preprint arXiv:1907.02057*, 2019.
- [15] S. Wang and K. Hauser, "Realization of a real-time optimal control strategy to stabilize a falling humanoid robot with hand contact," in *2018 IEEE International Conference on Robotics and Automation (ICRA)*, May 2018, pp. 3092–3098.
- [16] M. Chen and C. J. Tomlin, "Hamilton-jacobi reachability: Some recent theoretical advances and applications in unmanned airspace management," *Annual Review of Control, Robotics, and Autonomous Systems*, vol. 1, pp. 333–358, 2018.
- [17] M. Chen, Q. Hu, J. F. Fisac, K. Akametalu, C. Mackin, and C. J. Tomlin, "Reachability-based safety and goal satisfaction of unmanned aerial platoons on air highways," *Journal of Guidance, Control, and Dynamics*, vol. 40, no. 6, pp. 1360–1373, 2017.
- [18] M. Chen, J. F. Fisac, S. Sastry, and C. J. Tomlin, "Safe sequential path planning of multi-vehicle systems via double-obstacle hamilton-jacobisaisacs variational inequality," in *2015 European Control Conference (ECC)*. IEEE, 2015, pp. 3304–3309.
- [19] M. Chen, J. C. Shih, and C. J. Tomlin, "Multi-vehicle collision avoidance via hamilton-jacobi reachability and mixed integer programming," in *2016 IEEE 55th Conference on Decision and Control (CDC)*. IEEE, 2016, pp. 1695–1700.
- [20] J. Schulman, F. Wolski, P. Dhariwal, A. Radford, and O. Klimov, "Proximal policy optimization algorithms," *CoRR*, vol. abs/1707.06347, 2017.
- [21] I. Szita and A. Lőrincz, "Optimistic initialization and greediness lead to polynomial time learning in factored mdps," in *Proceedings of the 26th Annual International Conference on Machine Learning*, ser. ICML '09. New York, NY, USA: Association for Computing Machinery, 2009, p. 1001–1008. [Online]. Available: <https://doi.org/10.1145/1553374.1553502>
- [22] M. C. Machado, S. Srinivasan, and M. Bowling, "Domain-independent optimistic initialization for reinforcement learning," *ArXiv*, vol. abs/1410.4604, 2015.
- [23] B. Kim, A.-m. Farahmand, J. Pineau, and D. Precup, "Learning from limited demonstrations," in *Advances in Neural Information Processing Systems*, 2013, pp. 2859–2867.
- [24] J. Chemali and A. Lazaric, "Direct policy iteration with demonstrations," in *Twenty-Fourth International Joint Conference on Artificial Intelligence*, 2015.
- [25] J. Kober and J. Peters, "Imitation and reinforcement learning," *IEEE Robotics & Automation Magazine*, vol. 17, no. 2, pp. 55–62, 2010.
- [26] J. Kober, K. Mülling, O. Krömer, C. H. Lampert, B. Schölkopf, and J. Peters, "Movement templates for learning of hitting and batting," in *2010 IEEE International Conference on Robotics and Automation*. IEEE, 2010, pp. 853–858.
- [27] E. Greensmith, P. L. Bartlett, and J. Baxter, "Variance reduction techniques for gradient estimates in reinforcement learning," *Journal of Machine Learning Research*, vol. 5, no. Nov, pp. 1471–1530, 2004.
- [28] R. S. Sutton and A. G. Barto, *Reinforcement learning: An introduction*. MIT press, 2018.
- [29] L. Weaver and N. Tao, "The optimal reward baseline for gradient-based reinforcement learning," *arXiv preprint arXiv:1301.2315*, 2013.
- [30] J. Schulman, P. Moritz, S. Levine, M. I. Jordan, and P. Abbeel, "High-dimensional continuous control using generalized advantage estimation," *CoRR*, vol. abs/1506.02438, 2016.
- [31] C. Wu, A. Rajeswaran, Y. Duan, V. Kumar, A. M. Bayen, S. Kakade, I. Mordatch, and P. Abbeel, "Variance reduction for policy gradient with action-dependent factorized baselines," in *International Conference on Learning Representations*, 2018. [Online]. Available: <https://openreview.net/forum?id=H1tSsb-AW>
- [32] T. Zhang, G. Kahn, S. Levine, and P. Abbeel, "Learning deep control policies for autonomous aerial vehicles with mpc-guided policy search," in *2016 IEEE international conference on robotics and automation (ICRA)*. IEEE, 2016, pp. 528–535.
- [33] G. Kahn, T. Zhang, S. Levine, and P. Abbeel, "Plato: Policy learning using adaptive trajectory optimization," in *2017 IEEE International Conference on Robotics and Automation (ICRA)*. IEEE, 2017, pp. 3342–3349.
- [34] B. Ivanovic, J. Harrison, A. Sharma, M. Chen, and M. Pavone, "Barc: Backward reachability curriculum for robotic reinforcement learning," in *Proc. IEEE Int. Conf. Robotics and Automation*, 2019.
- [35] X. Lyu and M. Chen, "Ttr-based reward for reinforcement learning with implicit model priors," 2020.
- [36] R. S. Sutton, "Learning to predict by the methods of temporal differences," *Machine learning*, vol. 3, no. 1, pp. 9–44, 1988.
- [37] R. Bellman, "Dynamic programming and stochastic control processes," *Information and control*, vol. 1, no. 3, pp. 228–239, 1958.
- [38] N. Cesa-Bianchi, C. Gentile, G. Lugosi, and G. Neu, "Boltzmann exploration done right," in *Proceedings of the 31st International Conference on Neural Information Processing Systems*, ser. NIPS'17. Red Hook, NY, USA: Curran Associates Inc., 2017, p. 6287–6296.
- [39] Y. Pu, M. N. Zeilinger, and C. N. Jones, "Inexact fast alternating minimization algorithm for distributed model predictive control," in *53rd IEEE Conference on Decision and Control*, 2014, pp. 5915–5921.
- [40] H. Hu, Y. Pu, M. Chen, and C. J. Tomlin, "Plug and play distributed model predictive control for heavy duty vehicle platooning and interaction with passenger vehicles," in *2018 IEEE Conference on Decision and Control (CDC)*, 2018, pp. 2803–2809.
- [41] X. Lyu, "xlv mbb icra2021 appendix," accessed: 31-Oct-2020. [Online]. Available: https://github.com/SFU-MARS/SL_optCtrl/blob/master/xlv_MBB_ICRA2021_appendix.pdf
- [42] T. P. Lillicrap, J. J. Hunt, A. Pritzel, N. M. O. Heess, T. Erez, Y. Tassa, D. Silver, and D. Wierstra, "Continuous control with deep reinforcement learning," *CoRR*, vol. abs/1509.02971, 2016.
- [43] S. Fujimoto, H. Van Hoof, and D. Meger, "Addressing function approximation error in actor-critic methods," *arXiv preprint arXiv:1802.09477*, 2018.
- [44] P. Dhariwal, C. Hesse, O. Klimov, A. Nichol, M. Plappert, A. Radford, J. Schulman, S. Sidor, Y. Wu, and P. Zhokhov, "Openai baselines: high-quality implementations of reinforcement learning algorithms," 2019.

APPENDIX

A. System Dynamics of Planar Quadrotor

We use the following 6D ordinary differential equation to describe the evolution of the planar quadrotor:

$$\dot{\tilde{s}} = \begin{bmatrix} \dot{x} \\ \dot{y} \\ \dot{z} \\ \dot{\psi} \\ \dot{\omega} \end{bmatrix} = \begin{bmatrix} -\frac{1}{m}C_D^v v_x + \frac{F_1}{m} \sin \psi + \frac{F_2}{m} \sin \psi \\ -\frac{1}{m}(mg + C_D^v v_z) + \frac{F_1}{m} \cos \psi + \frac{F_2}{m} \cos \psi \\ -\frac{1}{I_{yy}}C_D^\psi \omega + \frac{1}{I_{yy}}F_1 - \frac{1}{I_{yy}}F_2 \end{bmatrix}, \quad (10)$$

where the quadrotor's movement is controlled by two motor thrusts, F_1 and F_2 . The quadrotor has mass m , moment of inertia I_{yy} , and half-length l . Furthermore, g denotes the gravity acceleration, C_D^v the translation drag coefficient, and C_D^ψ the rotational drag coefficient.

B. Reward Functions

We use Eq. (11) as the reward function for the two examples in Section V, where \mathbf{G} refers to the set of goal states, \mathbf{C} the set of collision states and \mathbf{I} the set of intermediate states which involves neither collision nor goal. Note that here s is the full MDP state, which includes both robotic internal states and sensor readings, for the target RL problem Ω .

Eq. (12) is used in Section VI for the Trap-Goal environment. Here, \mathbf{Tr} represents the states in the trap area.

$$r(s) = \begin{cases} 0 & s \in \mathbf{I} \\ +1000 & s \in \mathbf{G} \\ -400 & s \in \mathbf{C} \end{cases} \quad (11) \quad r(s) = \begin{cases} 0 & s \in \mathbf{I} \\ +1000 & s \in \mathbf{G} \\ +100 & s \in \mathbf{Tr} \\ -400 & s \in \mathbf{C} \end{cases} \quad (12)$$

C. Data Generation using MPC

1) *General MPC Formulation:* The goal of MPC for both examples is to generate trajectories from certain initial states to a desired goal region whilst avoiding obstacles. Using the point-mass optimization-based collision avoidance approach, the obstacle avoidance condition is:

$$\text{dist}(p, \mathbb{O}) > d_{min}, \quad (13)$$

where $\text{dist}(p, \mathbb{O}) := \min_t \{ \|t\|_2 : (p+t) \cap \mathbb{O} \neq \emptyset \}$. Then, p is the position of the point-mass, $d_{min} \geq 0$ is a desired safety margin with the size of real robot taken into account, and \mathbb{O} denotes a polyhedral obstacle which is a convex compact set with non-empty relative interior, represented as

$$\mathbb{O} = \{p \in \mathbb{R}^n : Ap \leq b\}, \quad (14)$$

where $A \in \mathbb{R}^{l \times n}$, $b \in \mathbb{R}^l$, l is the number of sides of the obstacle (in our example, all obstacles are shaped as cubes) and n is the dimensionality of positional states. Since (13) is non-differentiable, we reformulate the condition into an equivalent differentiable condition: $\text{dist}(p, \mathbb{O}) > d_{min} \iff \exists \lambda \geq 0 : (Ap - b)^\top \lambda > d_{min}, \|A^\top \lambda\|_2 \leq 1$, where λ is the dual variable. We now formulate the general MPC optimization problem as follows:

$$\begin{aligned} \min_{\tilde{s}, \tilde{a}, \lambda} & \sum_{k=0}^{H-1} \left((p_k - p_{ref})^\top \gamma^{k+1} Q (p_k - p_{ref}) + \tilde{a}_k^\top R \tilde{a}_k \right) \\ & + (p_H - p_{ref})^\top \gamma^{H+1} Q (p_H - p_{ref}) \\ \text{s.t.} & \tilde{s}_0 = \tilde{s}_{initial} \\ & \tilde{s}_{k+1} = \tilde{s}_k + T_s \tilde{f}(\tilde{s}_k, \tilde{a}_k), \quad \tilde{a}_k \in \Delta, \quad \forall k \in \{0, \dots, H-1\} \\ & \tilde{s}_k \in \tilde{S}, \quad \forall k \in \{0, \dots, H\} \\ & \tilde{s}_H \in \Gamma_3 \\ & \lambda_k^{(m)} \geq 0, \quad (A^{(m)} p_k - b^{(m)})^\top \lambda_k^{(m)} > d_{min}, \quad \|A^{(m)\top} \lambda_k^{(m)}\|_2 \leq 1, \\ & \forall m \in \{1, \dots, M\}, \quad \forall k \in \{0, \dots, H\} \end{aligned} \quad (15)$$

To match the notations in the main paper, here we employ \tilde{s} and \tilde{a} as the state and action of a low-dimensional model (as in Eq. (10)) used in MPC. Tilde indicates it is an approximate model \tilde{f} in contrast to the full MDP model f of the target RL problem. Specifically, H is the horizon length, $\tilde{s} = [\tilde{s}_0, \dots, \tilde{s}_H]$ is all the states over the horizon, $\tilde{a} = [\tilde{a}_0, \dots, \tilde{a}_{H-1}]$ is the actions over the horizon, $\lambda = [\lambda_0^{(1)}, \dots, \lambda_0^{(M)}, \lambda_1^{(1)}, \dots, \lambda_H^{(M)}]$ is the dual variables associated with obstacles $\mathbb{O}^{(1)} \dots \mathbb{O}^{(M)}$ over the horizon, M is the number of obstacles, \tilde{s}_k is the states at time k , p_k is the positional states at time k , p_{ref} is the reference position, \tilde{a}_k is the control inputs at time step k , γ is the scaling factor for the position error, Q is the weight matrix for the position error, R is the weight matrix for the control effort, $\tilde{s}_{initial}$ is the initial state, T_s is the sampling period, \tilde{f} is the continuous-time system dynamics, Δ is the collection of possible control inputs, \tilde{S} is the state constraints, Γ_3 is the collection of goal states, and $A^{(m)} \in \mathbb{R}^{l \times n}$ and $b^{(m)} \in \mathbb{R}^l$ define the obstacle $\mathbb{O}^{(m)}$ based on (14).

2) *Car Example MPC Formulation:* In the car scenario, the continuous-time system dynamics \tilde{f} is:

$$\dot{\tilde{s}} = \tilde{f}(\tilde{s}, \tilde{a}) = \begin{bmatrix} \dot{x} \\ \dot{y} \\ \dot{\theta} \end{bmatrix} = \begin{bmatrix} v \cos(\theta) \\ v \sin(\theta) \\ \omega \end{bmatrix} \quad (16)$$

where $\tilde{s} = [x, y, \theta]^\top$ and $\tilde{a} = [v, \omega]^\top$. In the optimization problem we have:

$$\begin{aligned} H &= 80; \gamma = 1.1; T_s = 0.05; d_{min} = 0.277; M = 6 \\ p &= [x, y]^\top; p_{ref} = [3.5, 3.5]^\top \\ Q &= \text{diag}([10, 10]^\top); R = \text{diag}([1, 1]^\top) \\ \Delta &= \{[v, \omega]^\top : -2 \leq v \leq 2, -2 \leq \omega \leq 2\} \\ \tilde{S} &= \{[x, y, \theta]^\top : |x| \leq 4.723, |y| \leq 4.723, -\infty \leq \theta \leq \infty\} \\ \Gamma_3 &= \{[x, y, \theta]^\top : \|[x, y]^\top - [3.5, 3.5]^\top\|_2 \leq 1, \cos(\theta - 0.75) \leq 0.3\} \end{aligned}$$

The matrices for specifying obstacles $\mathbb{O}^{(1)} \dots \mathbb{O}^{(6)}$ are:

$$\begin{aligned} A^{(m)} &= \begin{bmatrix} -1 & 0 \\ 1 & 0 \\ 0 & -1 \\ 0 & 1 \end{bmatrix}, \quad \forall m \in \{1, \dots, M\} \quad (17) \\ b^{(1)} &= \begin{bmatrix} 0.35 \\ 0.35 \\ 0.35 \\ 0.35 \end{bmatrix}, b^{(2)} = \begin{bmatrix} -2.65 \\ 3.35 \\ 1.35 \\ -0.65 \end{bmatrix}, b^{(3)} = \begin{bmatrix} -1.65 \\ 2.35 \\ -0.65 \\ 1.35 \end{bmatrix}, \\ b^{(4)} &= \begin{bmatrix} 2.35 \\ -1.65 \\ 2.35 \\ -1.65 \end{bmatrix}, b^{(5)} = \begin{bmatrix} 0.35 \\ 0.35 \\ -3.65 \\ 4.35 \end{bmatrix}, b^{(6)} = \begin{bmatrix} 3.35 \\ -2.65 \\ -1.65 \\ 2.35 \end{bmatrix}. \quad (18) \end{aligned}$$

3) *Quadrotor Example MPC Formulation:* In the quadrotor scenario, the continuous-time system dynamics \tilde{f} is denoted as Eq. (10). In the optimization problem we have:

$$\begin{aligned} H &= 140; \gamma = 1.1; T_s = 0.05; d_{min} = 0.1; M = 4 \\ p &= [x, z]^\top; p_{ref} = [4, 9]^\top \\ Q &= \text{diag}([10000, 10000]^\top); R = \text{diag}([1, 1]^\top) \\ \Delta &= \{[M_1, M_2]^\top : 5 \leq M_1 \leq 11, 5 \leq M_2 \leq 11\} \\ \tilde{S} &= \{[x, v_x, z, v_z, \phi, \omega]^\top : |x| \leq 4.75, 0.25 \leq z \leq 9.75, |\phi| \leq \pi/2\} \\ \Gamma_3 &= \{[x, z, \phi] : 3 \leq x \leq 5, 8 \leq z \leq 10, -\pi/3 \leq \phi \leq \pi/3\} \end{aligned}$$

In the quadrotor scenario, $A^{(m)}$ is the same as the car scenario in (17). However, $b^{(1)}, \dots, b^{(4)}$ are:

$$b^{(1)} = \begin{bmatrix} 3.25 \\ -0.75 \\ -3.75 \\ 6.25 \end{bmatrix}, \quad b^{(2)} = \begin{bmatrix} 1.25 \\ 1.25 \\ -7.5 \\ 9.5 \end{bmatrix}, \quad (19)$$

$$b^{(3)} = \begin{bmatrix} -1.75 \\ 5.75 \\ -3.75 \\ 6.25 \end{bmatrix}, \quad b^{(4)} = \begin{bmatrix} 0.75 \\ 0.75 \\ 0.5 \\ 2.5 \end{bmatrix}.$$

D. More results using TD(λ) return

As discussed in Sec. IV-C, the TD(λ) estimation of G_t^λ can include an on-policy value function $V^\pi(s_t)$ if $\lambda \in [0, 1)$. However, we demonstrate that our model-based baseline function $V^M(s_t)$ can not only act as a choice of the baseline function $b(s_t)$, but also a special, model-based value function for more general TD(λ) return to replace $V^\pi(s_t)$. Without the loss of generality, we test the cases where $\lambda = 0.95, 0.85$.

Fig. 4 illustrates the learning performance on the car and quadrotor examples respectively using our MBB approach⁴ with TD(λ) return, where $V^\pi(\cdot)$ is replaced by $V^M(\cdot)$. We observe similar data efficiency improvements as using Monte-Carlo return in Sec. V, which indicates the benefits of MBB approach under general TD(λ) return despite the potential bias. We also note that as λ decreases, the averaged policy performance decreases correspondingly in certain extent. This is potentially a possible negative effect of using $V^M(s_t)$ for TD(λ) estimation. Since $V^M(s_t)$ is calculated and approximated from a lower-dimensional problem, it introduces more bias than V^π in G_t^λ estimation. As λ decreases, such bias becomes more significant and can be more harmful to the learning process as the value function occupies larger proportion in the TD(λ) return.

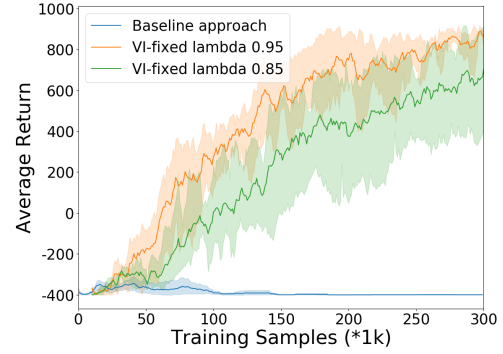
E. More Discussions

1) **Correctness of Policy Gradient Estimation:** Following the procedure in Section VI, we now further investigate the correctness of gradient estimation in the Trap-Goal environment. We take policies at certain iterations in the earlier learning stage and employ these policies to collect sample transitions from the Trap-Goal environment. Particularly, we denote $\pi_G^{20}, \pi_G^{40}, \pi_G^{60}$ as policies belong to the goal-reaching trials at iteration 20, 40, 60; $\pi_{Tr}^{20}, \pi_{Tr}^{40}, \pi_{Tr}^{60}$ as policies belong to the trap-reaching trials at iteration 20, 40, 60.

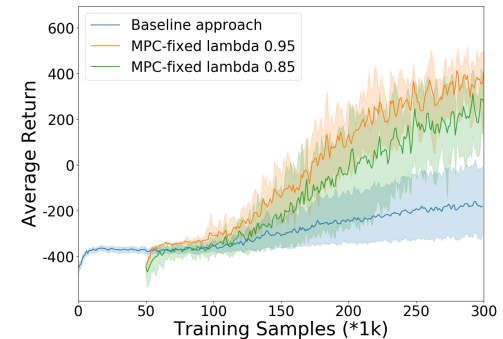
We first take Fig. 5a, 5b and 5c as a group to analyze the results since they are all using trap-reaching policies. In the three sub-figures, MBB approach always provide completely distinct gradient estimation from the baseline approach regardless of sample size or ground truth type (comparing blue, solid line to red, solid line, or blue, dashed line to red, dashed line). This suggests that MBB is capable of distinguishing the wrong policy optimization direction for the Trap-Goal task.

On the other hand, Fig. 5d, 5e and 5f show the cosine similarity for different sample sizes with the samples collected from goal-reaching policies. In this case, MBB and the baseline approach have consistent tendencies on gradient estimation. However, even in this case, our MBB approach still provides more accurate gradient estimation than the baseline approach (blue solid and dashed lines are mostly

⁴Specifically, we use VI-fixed as a representative variant of the MBB approach for the car and MPC-fixed for the quadrotor.



(a) Car example



(b) Quadrotor example

Fig. 4: Performance comparison between MBB and the baseline approach, where MBB approach uses TD(λ) return ($\lambda = 0.95, 0.85$) for policy gradient calculation.

above red solid and dashed lines respectively), especially at relatively lower sample sizes.

2) **Advantage Estimation:** We also investigate the advantage estimation to empirically show the efficacy of MBB algorithm. The advantage function $A^\pi(s, a)$ measures how much better an action a is than others on average, and has been extensively used in policy gradient algorithms to drive the policy update [30]. In this paper, we assume the advantage is defined by $A^\pi(s, a) = G_t^\lambda - b(s_t)$ as shown in Eq. (1) where $b(s_t)$ can be the on-policy value function $V^\pi(s_t)$ or our model-based baseline function $V^M(s_t)$.

Fig. 6a shows the advantage estimation comparison between MBB and the baseline approach. The total number of training iterations are 150 and we take an average of advantage estimation every 10 iterations. It is clearly observed that MBB approach maintains a relatively larger range of advantage estimation over the entire learning process. In contrast, the advantage estimation of the baseline approach gradually shrink to a very narrow range around zero. This may indicate that MBB involves more exploration thus more likely to escape local optima. On the other hand, as we already observed in the Fig. 1c, the baseline approach can often drive the robot get stuck in an undesired area for a long time due to the negligible advantage estimation.

3) **Variance of Policy Gradient Estimation:** We also conduct empirical analysis on the variance of gradient estimation. More specifically, at each training iteration, we

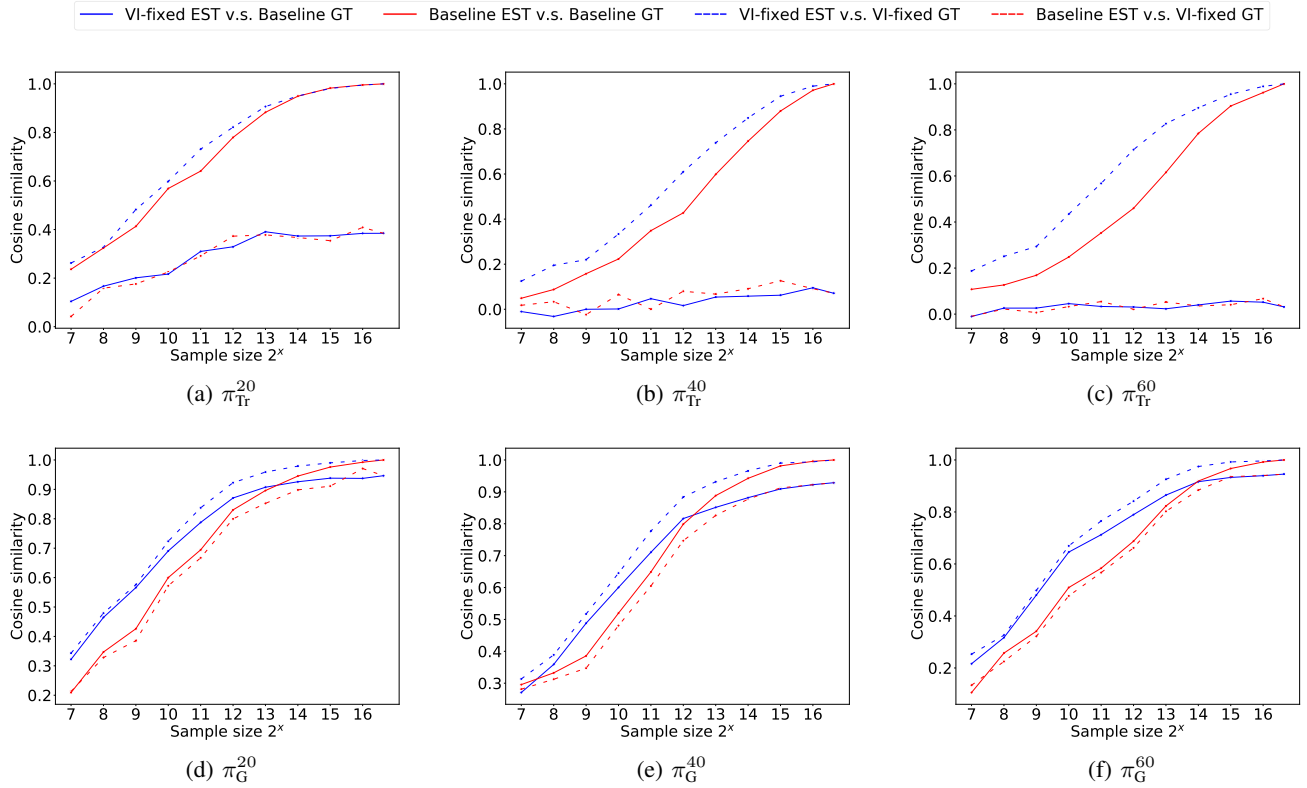


Fig. 5: The comparison on the correctness of policy gradient estimation between MBB and the baseline approach under varied sampling policies. We take (a), (b), (c) as a group, and (d), (e), (f) as another group to analyze. In each sub-figure, blue lines (solid or dashed) represent MBB-based gradient estimation with regard to different types of ground truths while red lines (solid or dashed) represent that of the baseline approach. A good comparison group would be “blue solid v.s. red solid” or “blue dashed v.s. red dashed”.

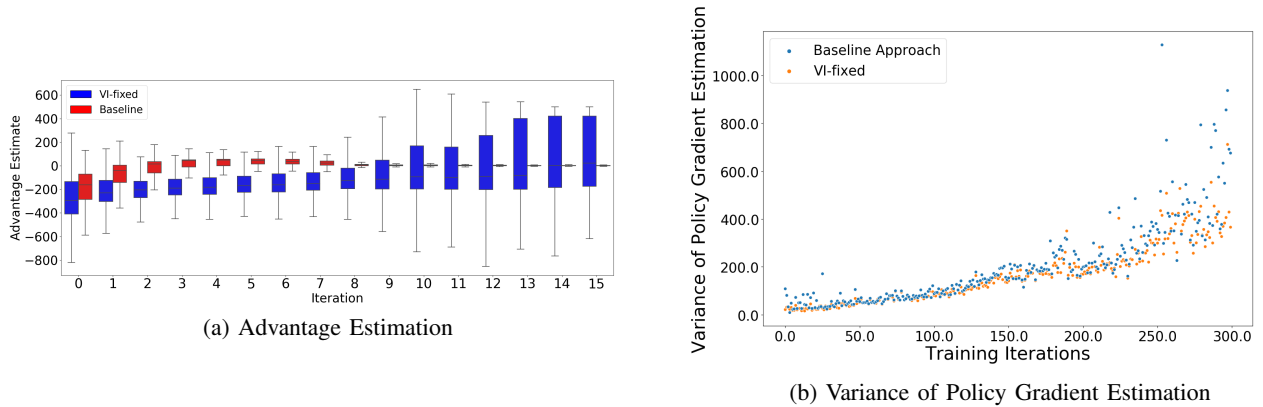


Fig. 6: (a) Advantage estimation versus training iterations using MBB and the baseline approach. Larger colored box refers to wider range of advantage estimation. (b) Policy gradient variance computed via MBB and the baseline approach. Each dot corresponds to the magnitude of variance at certain iteration.

collect K^5 samples with each of them denoted as $D_i = (s_i, a_i, r_i, s_{i+1}); i \in \{0, 1, 2, \dots, K\}$ using MBB and the baseline approach respectively and calculate K policy gradients $\nabla_{\theta} J(\theta|D_i)$ based on each sample. Then we compute the largest singular value of co-variance matrix of each set of gradients $\{\nabla_{\theta} J(\theta|D_i) \mid i \in \{0, 1, \dots, K-1\}\}$.

Fig. 6b shows the gradient variance magnitude versus training iterations. MBB (orange dots) and the baseline (blue dots) approach share comparable variance of gradient estimation over the entire training process. This fully shows the benefits of our MBB approach since our model-based baseline are facilitating the learning performance by providing necessary exploration and better gradient direction whilst not introducing too much variance.

F. Results on Q-learning based Algorithm

In contrast to direct policy gradient based methods (like PPO), Q-learning based methods are another important type of model-free RL algorithms. Deep Deterministic Policy Gradient (DDPG) algorithm is a well-known example. Unlike PPO which directly executes policy gradient optimization, DDPG first learns an on-policy Q function $Q^{\pi}(s, a)$ and then derives a policy based on $Q^{\pi}(s, a)$ [42].

We test our MBB approach on a refined DDPG algorithm (known as TD3 [43]) to demonstrate its compatibility and efficacy on different types of model-free RL algorithms.

1) **Important Procedure of DDPG Algorithm:** In DDPG, the Q function $Q^{\pi}(s, a)$ is often represented by a nonlinear function approximator (e.g. neural network) with parameters ϕ , denoted as $Q_{\phi}^{\pi}(s, a)$. Here we simplify $Q_{\phi}^{\pi}(s, a)$ to $Q_{\phi}(s, a)$ for conciseness. In addition, a Q target function $Q_{\phi_{\text{target}}}(s, a)$ is introduced in order to alleviate the optimization instability [42]. At each iteration, the Q target function $Q_{\phi_{\text{target}}}(s, a)$ is also responsible for providing the Q function approximation target $y(r, s', d)$:

$$y(r, s', d) = r(s) + \gamma(1-d)Q_{\phi_{\text{target}}}(s', \mu_{\theta_{\text{target}}}(s')) \quad (20)$$

where $\mu_{\theta_{\text{target}}}$ is the parameterized target policy. Then Q function $Q_{\phi}(s, a)$ is updated towards $y(r, s', d)$ by one-step gradient descent using Eq. (21) where \mathcal{B} is a batch of transition data sampled from original RL problem Ω :

$$\phi \leftarrow \phi - \alpha \nabla_{\phi} \frac{1}{|\mathcal{B}|} \sum_{(s,a,r,s',d) \in \mathcal{B}} (Q_{\phi}(s, a) - y(r, s', d))^2 \quad (21)$$

The policy μ_{θ} is updated subsequently via one-step gradient ascent towards $Q_{\phi}(s, a)$ via:

$$\theta \leftarrow \theta + \beta \nabla_{\theta} \frac{1}{|\mathcal{B}|} \sum_{s \in \mathcal{B}} Q_{\phi}(s, \mu_{\theta}(s)) \quad (22)$$

α and β are step sizes. The Q target $Q_{\phi_{\text{target}}}(s, a)$ and policy target $\mu_{\theta_{\text{target}}}$ then need to be updated in certain way such as polyak averaging:

$$\begin{aligned} \phi_{\text{target}} &\leftarrow \rho \phi_{\text{target}} + (1-\rho)\phi \\ \theta_{\text{target}} &\leftarrow \rho \theta_{\text{target}} + (1-\rho)\theta \end{aligned} \quad (23)$$

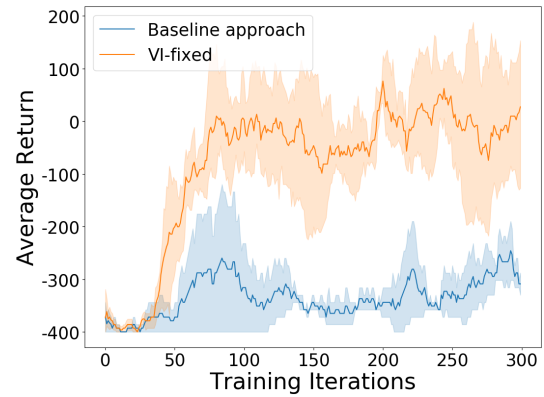
⁵We use $K = 1024$ at each training iteration

2) **MBB-based DDPG Algorithm:** We take ‘‘VI-fixed’’ as the representative variant of our MBB algorithm and integrate it into DDPG via the following two steps:

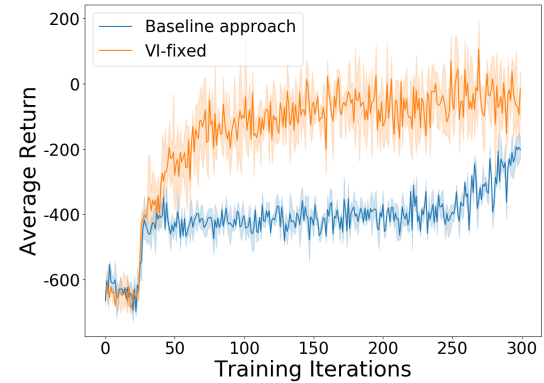
- 1) Our model-based baseline function $V^M(\cdot)$ can be considered as a special value function which contains the model information from a simplified, low-dimensional problem. Therefore, we can use $V^M(\cdot)$ and one-step simulation to replace $Q_{\phi_{\text{target}}}(s, a)$ in Eq. (20), where the one-step simulation is shown as Eq. (24) assuming a deterministic full MDP model.

$$Q_{\phi_{\text{target}}}(s, a) = r(s) + \gamma V^M(s') \quad (24)$$

- 2) The variant ‘‘VI-fixed’’ does not enable the subsequent update of $V^M(\cdot)$. Correspondingly, we can disable the update of $Q_{\phi_{\text{target}}}(s, a)$ in Eq. (23).



(a) Car Example



(b) Quadrotor Example

Fig. 7: Overall learning performance comparison using MBB-based and the original TD3 algorithms on two robotic examples. We take the averaged training return versus training iterations as performance measurement. Results are summarized across 5 different trials. The curves show the mean return and the shaded area represents the standard deviation of 5 trials.

Particularly in TD3 algorithm, there are two Q target functions: $Q_{\phi_{\text{target},1}}(s, a)$ and $Q_{\phi_{\text{target},2}}(s, a)$, and $y(r, s', d)$ is computed by:

$$y(r, s', d) = r(s) + \gamma(1-d) \min_{i=1,2} Q_{\phi_{\text{target},i}}(s', a'(s')) \quad (25)$$

Therefore, with MBB, we simply use $V^M(\cdot)$ and Eq. (24) to replace both Q target functions $Q_{\phi_{\text{target},1}}(s, a)$ and $Q_{\phi_{\text{target},2}}(s, a)$ and disable the update of them.

Fig. 7 illustrates how the learning progresses with MBB-based and the original TD3 algorithm (noted as the baseline approach) on two robotic problems in Section V. Note that the baseline approach uses random initialized Q target function and regular Q target update following Eq. (23). MBB approach refers to a new TD3 algorithm that involves the refinement described in this section. As evident from Fig. 7, MBB approach continues to improve the policy with tolerable variance, and outperforms the baseline approach at around 50 iterations on both examples. For the quadrotor case, even though the baseline approach eventually improves at around 280 iteration, it largely lags behind MBB approach and shows poor data efficiency.

G. Code base and hyper-parameters of neural networks

For the PPO algorithm, we follow the implementations from OpenAI Baselines [44]. For the TD3 algorithm, we follow the original implementations from the author. Table. II summarizes the neural network structure as well as the main hyper-parameters of PPO and TD3 algorithm.

	PPO	TD3
Type of layers	FC	FC
Structure of layers	(64,64)	(256,256)
Total timesteps	300K	300K
Policy clipping	0.2	×
Learning rate	$3e^{-4}$	$1e^{-3}$
SGD Optimizer	Adam	Adam
Discount γ	0.998	0.99
λ for TD(λ) return	[1, 0.95, 0.85]	×
Gradient clipping	0.5	×
Policy noise	×	0.2
Policy update frequency	×	2
Target network update rate	×	0.005

TABLE II: Main hyper-parameters and neural network structures for PPO and TD3 algorithm.